



# Fabrication and investigation of effect of core size in heterostructure PbS/CdS core/shell nanoparticles

D. Das<sup>1</sup> · A. M. P. Hussain<sup>1</sup>

Received: 30 November 2017 / Accepted: 13 March 2018 / Published online: 16 March 2018  
© Springer-Verlag GmbH Germany, part of Springer Nature 2018

## Abstract

PbS/CdS core/shell (CS) nanoparticles (NPs) were fabricated with three different concentrations of PbS core and CdS shell. Formation of core/shell heterostructure was confirmed from X-ray diffraction studies. The diffraction patterns exhibited formation of cubic phase and polycrystalline core/shell nanostructure. The crystalline sizes calculated from Williamson–Hall plot exhibited increase with molar concentration of precursors with decrease in strain. High resolution electron microscopy studies also confirm the formation of core/shell structure with particle size around 10 nm. A large blue-shift for PbS core compared to its bulk and small red-shift for the PbS/CdS core/shell as compared to the core is being observed in absorption spectra.

## Abbreviations

NPs	Nanoparticles
QDs	Quantum dots
MEG	Multiple exciton generation
CS	Core/shell
CBD	Chemical bath deposition
XRD	X-ray diffraction
SAED	Selected area electron diffraction
HRTEM	High resolution transmission electron microscopy
FWHM	Full width half maximum
W–H	Williamson–Hall
$\alpha$	Absorption coefficient

a distinct absorption spectrum with large blue-shift as compared to their bulk structure. PbS is an IV–VI semiconductor with a cubic rock salt structure having a narrow band gap of 0.41 eV for which even at shorter wavelength they show continuous optical absorption. PbS shows multiple exciton generation (MEG) where a single photon produces two or more excitons. This aids in the construction of solar cells with higher photo conversion efficiency as much as 66% [9]. It plays a pivotal role in photovoltaic application and biosensors [10]. CdS is a II–VI semiconductor with wurtzite structure having a band gap of 2.49 eV. The band gap of CdS is suitable as a shell material for the absorption of solar light. It is largely used as window material in biological field, in the constructing solar cell and other photo voltaic devices.

Applications of semiconductor NPs have been largely hindered as most of the NPs are toxic, bio-incompatible, unstable under ambient environment and has uncontrolled crystal growth due to agglomeration of NPs. PbS, CdS nanoparticles are hydrophobic, unstable due to uncontrolled crystal growth and are not environmental friendly. The use of biological capping materials is gaining importance over these limitations because of their nontoxic and environment friendly nature [11]. But biological capping cannot passivate both cationic and anionic type of free charges. The dangling bonds present on the surface of NPs result in reduced optical activity. Epitaxial growth of few monolayers of inorganic shell over core NPs are capable of passivating both types of free ions and dangling bonds that can stabilize the NPs. Such a NP, encapsulated by few monolayers of an inorganic material where the core property predominates is known as core/shell (CS) NPs. Inorganic shell along with biological

## 1 Introduction

Semiconductor nanoparticles (NPs) has drawn interest across the globe for their size tunable optical properties. PbS and CdS semiconductor NPs have diverse applications such as photovoltaic [1, 2], biosensors, bio-marker, bio-labelling [3], and solar energy harvesting [4, 5]. The size dependent optical properties arise from strong quantum confinement effect [6–8], when the particle size goes below the Bohr exciton radii. The small size semiconductor quantum dots (QDs) such as PbS, CdS with their narrow size distribution exhibit

✉ D. Das  
ddasphy014@gmail.com

<sup>1</sup> Department of Physics, Cotton University, Guwahati, Assam 781001, India

capping of organic ligand such as starch, glycerol, DNA, L-cystrain, etc. make nanoparticles hydrophilic and environmentally stable. The biological capping materials can be modified, engineered or re-designed to act as bio linker for the use of nanocrystals as bio-sensors and bio-marker [12].

In the present work, PbS/CdS CS NPs of different shell thickness with glycerol as a capping material have been synthesized. Although a large number of works has been reported on PbS and CdS NPs separately, PbS/CdS CS NPs has not been explored much. The structural morphologies and optical properties of the synthesized PbS/CdS CS NPS has been investigated and reported in this communication.

## 2 Experimental details

The CS NPs has been synthesised using simple, low cost, single pot chemical bath deposition (CBD) technique which is suitable for large scale synthesis. The precursors glycerol, lead acetate, cadmium acetate, lead acetate, thiourea, ammonia with 99.9% purity were used as received from Sigma–Aldrich.

To fabricate PbS/CdS CS NPs, we first prepared the core material PbS NPs. 30 mM lead acetate and 30 mM thiourea solutions were separately prepared with double distilled water. Aqueous solution of 5% glycerol was prepared with double distilled water at 30 °C and stirred thoroughly in a round bottom flask. The pH of the lead acetate solution was maintained between eight and nine by adding NH<sub>4</sub>OH. 30 mM lead acetate solution was added drop wise to the glycerol solution under constant stirring. 30 mM thiourea solution was added to the reaction vessel drop wise and then stirred for 6 h at 30 °C to obtain dark brown PbS NPs.

To grow CdS shell over the freshly fabricated PbS NPs, 3 mM cadmium acetate and 3 mM thiourea solutions were prepared separately with double distilled water. These two solutions were then alternately added to the PbS NP solution in the step of 1 mL under constant stirring. The mixture was then kept under vigorous stirring for 10 h at constant temperature. Then the mixture was kept under reflux conditions for 5 h. The obtained nanoparticles were then filtered and washed with double distilled water for further characterization. With this protocol we had prepped PbS/CdS CS NPs with three different core concentration (A) 30 mM, (B) 50 mM and (C) 70 mM along with three shell concentration that was ten times less than the core concentration, i.e. 3, 5 and 7 mM. The structural and optical properties of all these samples were swot up with different characterisation techniques.

X-ray diffraction (XRD) pattern of the particles deposited at different temperatures were recorded with an X-Ray Diffractometer (XRD 3003 TT) in the  $2\theta$  range (20°–70°)

using Cu radiation of wavelength 1.541 Å and accelerating voltage 200 kV. The images of structural morphology and corresponding selected area electron diffraction (SAED) patterns of PbS/CdS CS NPs were taken using a high resolution transmission electron microscopy (HRTEM, JEOL-JEM-2100). The optical absorption spectra of the powder were measured in the wavelength range 200–900 nm using a spectrophotometer (CECIL-7500 Scan UV–Visible spectrophotometer) at room temperature. Photoluminescence measurements of the samples were made by a spectrophotometer (F-2500 FL) in the range of 400–800 nm, using excitation wavelength 250 nm.

## 3 Result and discussion

### 3.1 Structural studies

XRD patterns for the PbS/CdS CS NPs with different core concentrations (A) 30 mM, (B) 50 mM and (C) 70 mM are shown in Fig. 1. The trace of XRD patterns exhibit polycrystalline nature with face-centred cubic rock salt structure as confirmed from JCPDS data (file no: 78-1901). The rock salt structure is quite common in chemically synthesized lead sulphide [6, 8]. Diffraction peak broadening confirms the formation of nano-sized particles in the materials. No extra peaks for CdS were detected in the XRD pattern confirming the formation of PbS/CdS CS structure, not an alloy. The crystalline sizes (Table 1) of the fabricated nanocrystals are estimated using Scherer's formula.

$$D = K\lambda/\beta \cos \theta \quad (1)$$

where  $\beta$  is the full width at half maximum (FWHM) of the diffraction peak. Lattice constant ( $a$ ) of PbS particles for each diffraction line were calculated with the relation [13]

$$a^2 = d^2 (h^2 + k^2 + l^2) [\text{Å}] \quad (2)$$

where  $h$ ,  $k$  and  $l$  are the Miller indices. The average crystalline sizes of the PbS core nanoparticles with core concentration 30, 50 and 70 mM and different shell thickness are shown in Table 1. The crystalline sizes of the core/shell NPs were found to increase with increased core concentration as well as shell thickness. The lattice constant of the synthesized PbS NCs were found (Table 1) slightly different from their bulk value 5.936 Å which can be attributed to strain or microstrain in the nanocrystallites [14]. The non-uniform strain in the sample also contribution to the diffraction peak broadening; however, it may be a small fraction [14]. Thus, the sizes of the nanocrystals calculated using Scherer formula are slightly more than their actual sizes. Williamson–Hall (W–H) plot gives a better estimation for size and strain of the nanocrystals as compared to those given by Scherer formula because of the small variation of

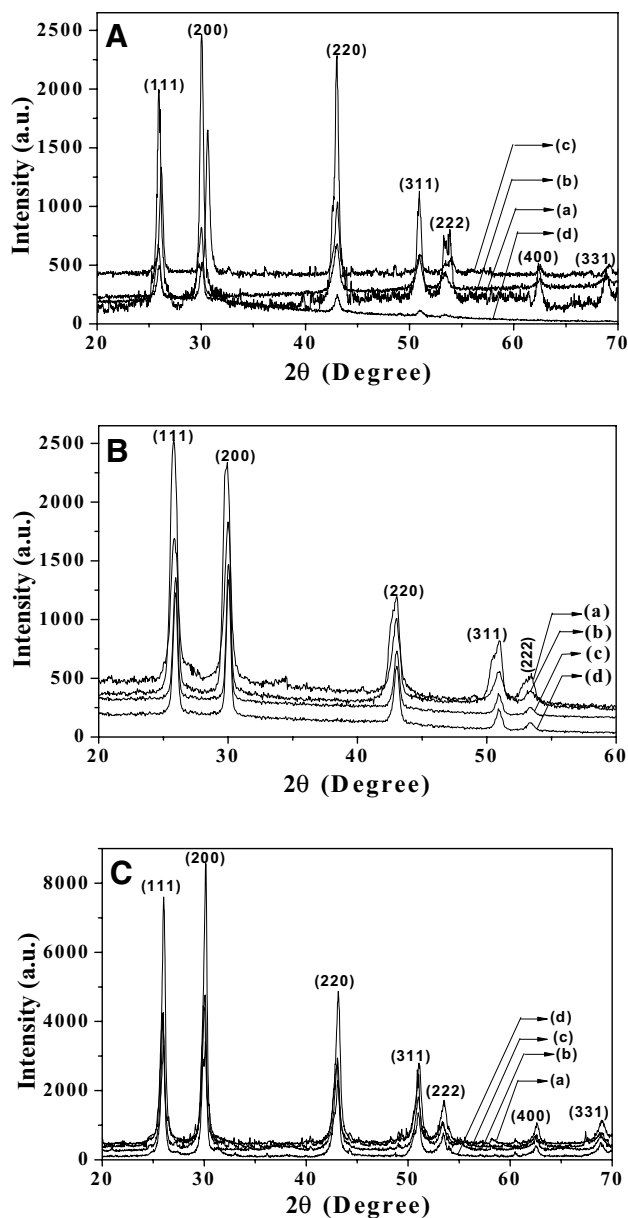


**Fig. 1** XRD pattern of PbS/CdS core/shell Nps synthesized at core concentrations (a) 30 mM, (b) 50 mM and (c) 70 mM with shell concentrations of (a) 3 mM, (b) 5 mM, (c) 7 mM and (d) core only

lattice constant from the standard JCPDS. The average size and strain of the nanocrystals are obtained from W–H plot based on the relation:

$$\beta \cos \theta = k \cdot \lambda / D + 4\epsilon \sin \theta \tag{3}$$

where  $\epsilon$  is the strain and  $k$  a constant.

The strain of the nanocrystals induced due to crystal imperfection and distortion, which can be calculated using the relation [15]

$$\epsilon = \beta / 4 \sin \theta \tag{4}$$

Figure 2 shows the Williamson–Hall (W–H) plot for PbS/CdS CS NPs synthesis at three molar concentration of core as (A) 30 mM, (B) 50 mM and (C) 70 mM. The plot between  $\beta \cos \theta / \lambda$  and  $4 \sin \theta / \lambda$  gives a straight line. The inverse of intercept gives the crystalline size of the nanocrystals while strain can be calculated from the slope of the graph. The average crystallite sizes and strain in the sample as obtained from W–H plot are shown in Table 1. The strain in CS NPs is influenced by two factors, (1) the curvature of the NPs and (2) thickness of the shell. When the particle sizes grows, the curvature decreases and hence the strain [16]. But increased shell thickness increases stress on the core resulting in increase in strain. The strain at smaller size of core NPs is higher which exhibits a decreasing trend with increase in size and the decrease in strain is attributed to lesser curved surface [17] at larger particle size. Variation of strain with crystalline size shown in Fig. 3. In CS with smallest core sizes, the strain initially increases with smaller shell thickness which may be attributed to the strain exerted by the shell materials and the same reduces with higher shell thickness because of reduced curvature [17] at larger particle dimension. The strain at smaller dimension is higher and initial shell growth exerts more stress resulting in increase in strain which gets relaxed at comparatively larger CS size due to reduced surface curvature. In the mid-sized NPs, the strain also lies in between which shows decreasing with increased shell because of reducing curvature and the stress of increased shell gets nullified by the relaxation due to decreased curvature. The strain of the largest core, with comparatively lesser curved surface, is smaller which increases with shell thickness as thicker shell exerts more stress and the relaxation of strain due to lesser curved surface is not dominating here. From this observation, it can be inferred that the fabricated NPs are spherical in shape. W–H plot is a typical linear fit of the data, but because of the existence of anisotropic variation in the residual strain, we cannot fit the experimental data exactly in a straight line [14].

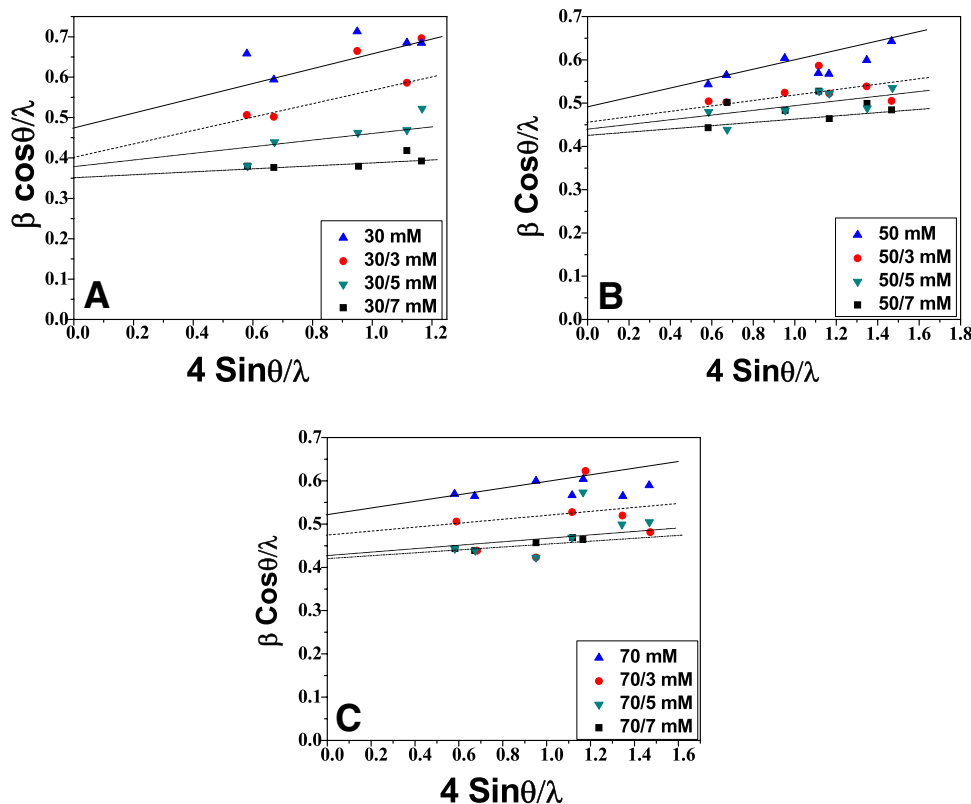
### 3.2 Electron microscopy

Representative HRTEM images of PbS/CdS CS NPs with concentrations (A) 70/5 mM, (B) 50/5 mM and (C) 30/3 mM are shown in Fig. 4. The resultant QDs are basically spherical shaped with a uniform size distribution of an average particle size of ~10 nm. Figure 4d shows the  $d$  spacing for core and shell for PbS/CdS CS NPs and it is found that the  $d$  value for PbS core is 0.18 nm and CdS shell is 0.32 nm. The different  $d$  values of PbS and CdS semiconductor shown in Fig. 4d confirmed that they do not overlap. Figure 4c, d also confirms the formation of core/shell structure nanoparticles. However, a close observation of HRTEM micrograph reveals that CS NPs are agglomerated with very narrow separation. Agglomeration is quite unavoidable in colloidal matrix

**Table 1** Structural parameters of PbS core and optical parameters of Glycerol capped PbS/CdS core/shell nanoparticles

Sample	Molarities (mM)	Size measured from		Strain	Lattice constant (a) [Å]	Absorption wavelength λ (nm)	Energy band gap E <sub>g</sub> (eV)
		Scherrer formula	W-H plot				
PbS	30	10	4.3	0.1520	5.1429	473	4.5
PbS/CdS	30/3	10	4.6	0.1693	5.1363	482	4.4
"	30/5	12	5.6	0.2245	5.1547	484	3.8
"	30/7	14	6.2	0.0511	5.1529	488	3.5
PbS	50	12	4.4	0.1155	5.1547	480	3.90
PbS/CdS	50/3	14	5.8	0.1054	5.1529	485	3.21
"	50/5	14	6.7	0.0754	5.1547	496	3.76
"	50/7	14	8.3	0.0498	5.1547	498	2.97
PbS	70	13	6.6	0.0531	5.1547	485	3.89
PbS/CdS	70/3	15	9.1	0.1623	5.1429	488	3.84
"	70/5	15	9.9	0.2233	5.1547	492	3.79
"	70/7	15	10.8	0.3151	5.1429	497	3.71

**Fig. 2** Williamson–Hall plot for PbS/CdS core/shell nanoparticles synthesized with core concentrations (a) 30 mM, (b) 50 mM and (c) 70 mM. Core alone (blue up triangle) 3 mM (red filled circle), 5 mM (green filled down triangle) and 7 mM (filled square) represents the shell concentrations, respectively, over the corresponding core nanoparticles



solution [18]. So usually the particle size measurement is not well in agreement with XRD. SAED pattern of PbS/CdS CS NPs shows the prominent planes of the respective material that also appeared in X-ray diffractogram.

### 3.3 Optical absorption studies

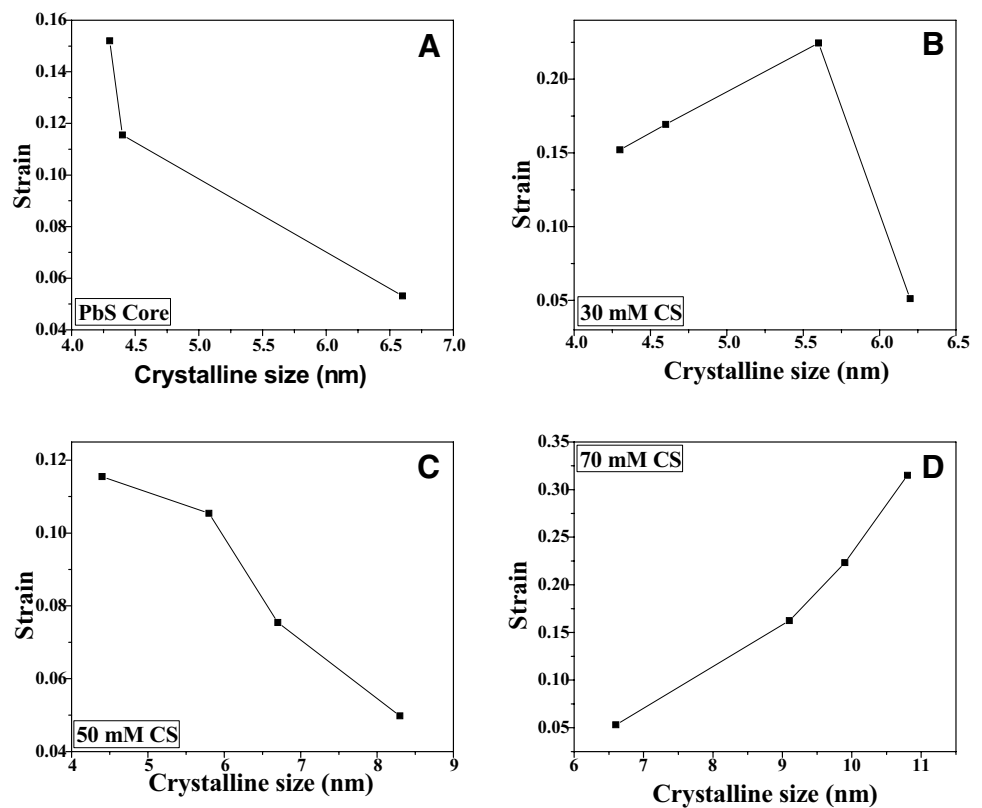
The electron excitation from the valence band to the conduction band that corresponds to the fundamental absorption

can be used to determine the nature and the value of the optical band gap. The relation between absorption coefficient ( $\alpha$ ) and the independent photon energy ( $h\nu$ ) can be written as [19]

$$(\alpha h\nu)^{1/n} = A(h\nu - E_g) \tag{5}$$

where  $A$  is a constant,  $E_g$  is the band gap of the material and exponent  $n$  depends on the type of transition. The

**Fig. 3** Variation of strain with crystalline size for (a) PbS core alone and PbS/CdS core/shell NPs with (b) 30 mM, (c) 50 mM and (d) 70 mM PbS core with different shell concentration



values of  $n$  are  $1/2$ ,  $2$  and  $3/2$  for direct allowed, indirect allowed and forbidden transmission, respectively. Figure 5 shows the absorption spectra for PbS/CdS CS NPs. The absorption coefficient ( $\alpha$ ) is calculated by absorbance data from UV–Vis absorption spectra without taking into consideration of scattering phenomenon. The band gaps are achieved from the linear portion of the Tauc's plot  $(\alpha h\nu)^2$  vs  $h\nu$  plot as shown in Fig. 6. Due to strong quantum confinement effect, the direct band gap of PbS/CdS CS NPs are increases from their bulk value (0.41 eV). It is reported that the size of the NPs along with their structure effect on controlling the band gap of the NPs. This is because when the size of the particle decreases till the nano range, the decrease in confine dimension makes the energy levels discrete and this increase or widen up the band gap. Ultimately the band gap energy also increases. Since the band gap and wavelength are inversely related to each other, the wavelength increase with decrease in size [20]. With increase in molar concentration of core material as well as shell material results in the increase in particle size. A red shift occurs in the absorption spectra from 342 to 384 nm and decrease in band gap from 4.5 to 2.97 eV (Table 1). The observed redshift of the absorption spectra can be attributed to the formation of thicker shell [17] around PbS NPs, which presumably exerts stress on

the NPs. This confirms that the size of CS NPs increases with increase in precursor concentration.

## 4 Conclusion

XRD results confirmed the cubic phase and polycrystalline nature of PbS/CdS CS NPs that were synthesized by CBD method. XRD patterns showed no extra pick for shell material which was also confirmed from the SEAD pattern. This means that pure CS NPs were formed. Slightly pick shift arises due to strain. The strain value decreases as crystalline size increases when the molar concentration of the nanocrystals was increased. HRTEM provide direct proof of the formation of PbS/CdS CS NPs with size around 10 nm. The UV–Vis absorption studies show that the direct band gaps lay in the range 2.97–4.40 eV. This estimated band gap values are much higher than their bulk value that are attributed to quantum confinement of the carriers in the nanocrystals. According to UV–Vis absorption, the optical characteristics observed in the synthesized PbS/CdS Core/shell material that has a higher confinement effect and pure core/shell NPs form. This Glycerol capped PbS/CdS CS NPs have scope for application in biomarker.



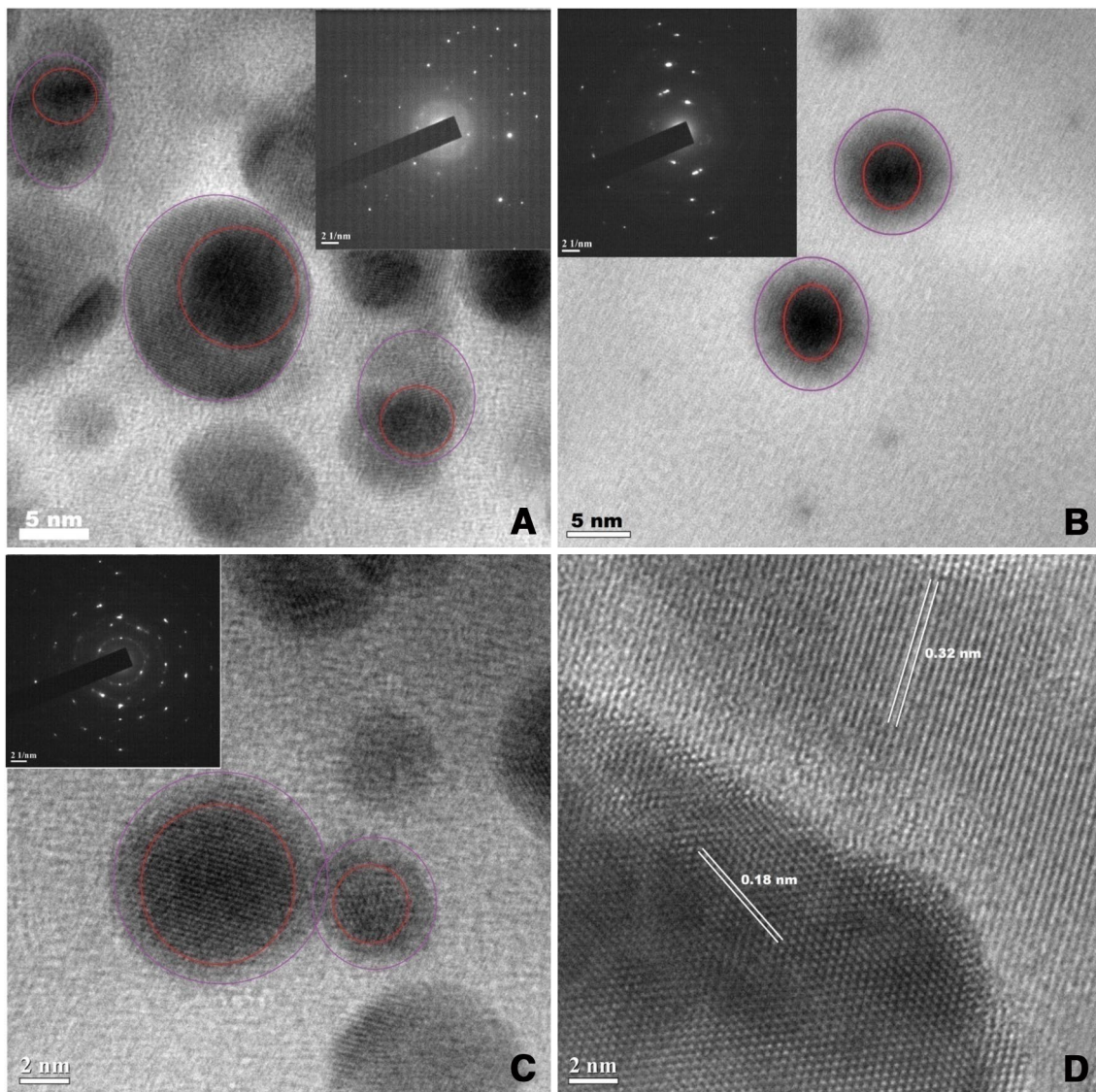


**Fig. 4** HRTEM images of PbS/CdS core/shell NPs synthesized at core concentration (a) 30 mM, (b) 50 mM and (c) 70 mM with 5 mM shell concentration and (d) *d* spacing for PbS/CdS CS NPs

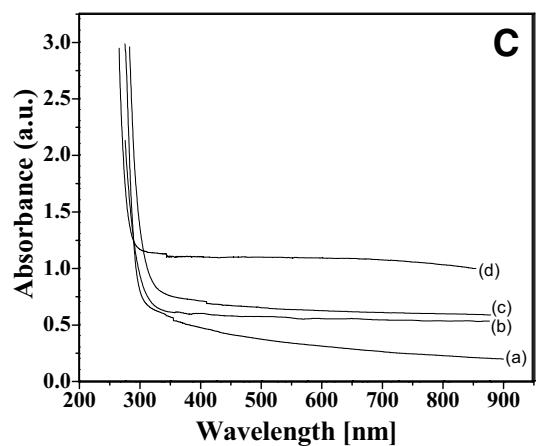
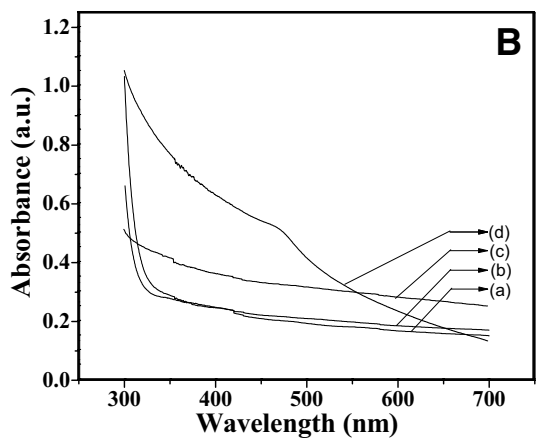
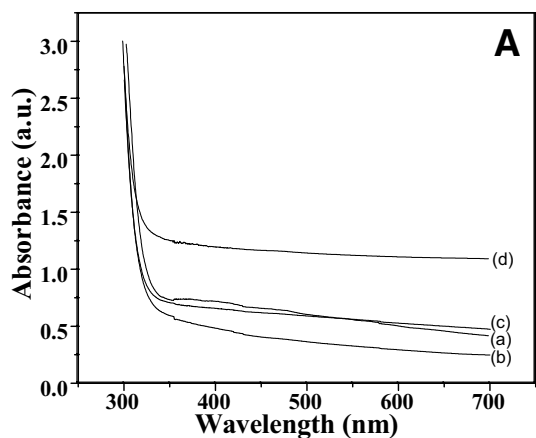


**Fig. 5** UV-Vis absorption spectra for PbS/CdS core/shell Nps synthesized at core concentration (a) 30 mM, (b) 50 mM and (c) 70 mM with shell concentrations of (b) 3 mM, (c) 5 mM, (d) 7 mM and (a) core only

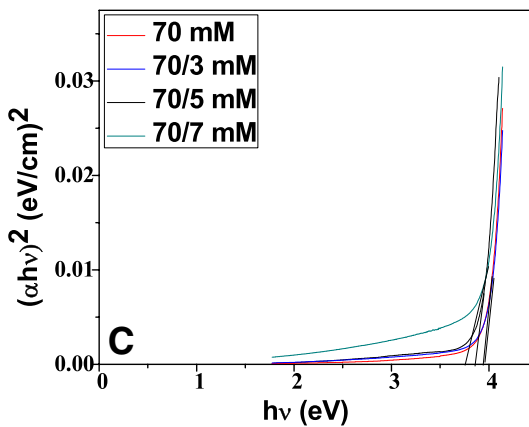
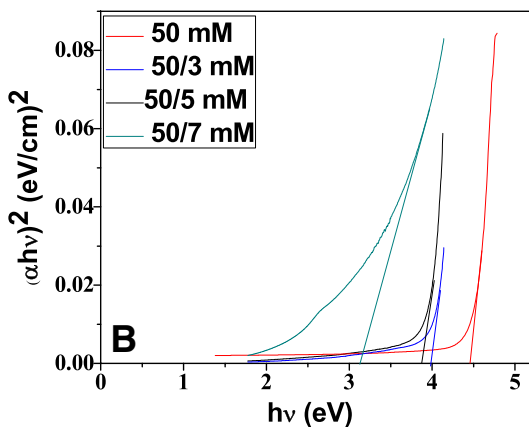
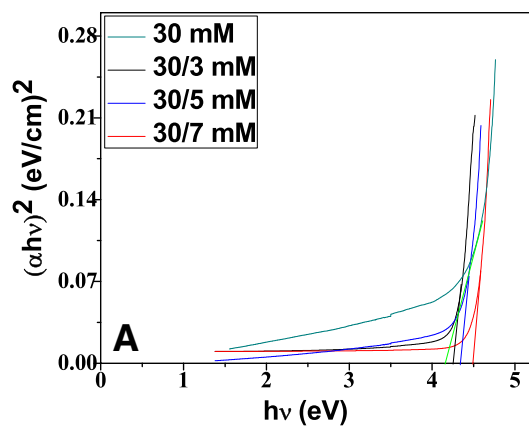


**Fig. 6** Tauc's plot for PbS/CdS core/shell Nps synthesized at core concentration of (a) 30 mM, (b) 50 mM and (c) 70 mM

**Acknowledgements** We acknowledge department of Physics, IIT Guwahati for providing facility of XRD measurements and SAIF, NEHU, Shillong for providing facility of HRTEM. I would also like to thanks CSIR-HRDG for JRF Grant [08/446(0001)2014-EMR-1].

## References

1. K.P. Acharya, N.N.H. Kasakarage, T.R.A.I. Nemitz, E. Khon, B. Ullrich, P. Anzenbacher, M. Zamkov, *J. Phys. Chem. C* **114**(29), 12496–9 (2010)
2. K. Das, S.K. De, *J. Phys. Chem. C* **113**, 3494 (2009)
3. M.J. Bruchez, M. Moronne, P. Gin, S. Weiss, A.P. Alivisatos, *Science* **281**(5385), 2013 (1998)
4. N. Zhao, T.P. Osedach, L.Y. Chang, S.M. Geyer, D. Wanger, M.T. Binda, A.C. Arango, M.G. Bawendi, V. Bulovic, *ACS Nano* **4**(7), 3743 (2010)
5. M. Shalom, S. Dor, S. Ruhle, L. Grinis, A. Zaban, *J. Phys. Chem. C* **113**(9), 3895 (2009)
6. K. Moreels, D. Lambert, D.D. Smeets, T. Muynck, J.C. Nollet, F. Martins, A. Vanhaecke, C. Vantomme, G. Delerue, Z. Allan, Hens, *ACS Nano* **3**(10), 3023 (2009)
7. X. Shen, Z. Li, Y. Cui, Y. Pang, *Int. J. Electrochem. Sci.* **6**, 3525 (2011)
8. F.W. Wise, *Acc. Chem. Res.* **33**(11), 773 (2000)
9. J. Akhtar, M.A. Malik, P. O'Brien, K.G.U. Wijayantha, R. Dharmadasa, S.J.O. Hardman, D.M. Graham, B.F. Spencer, S.K. Stubbs, W.R. Flavell, D.J. Binks, F. Sirrotti, E. Kazzi, M. Silly, *J. Mater. Chem.* **20**, 2336 (2010)
10. Y. Li, L. Wei, X. Chen, R. Zhang, X. Sui, Y. Chen, J. Jiao, L. Mei, *Nanoscale Res. Lett.* **8**, 67 (2013)
11. N. Ma, J. Yang, K.M. Stewart, S.O. Kelley, *Langmuir* **23**(26), 12783 (2007)
12. S.N. Sarangi, S.N. Sahu, S. Nozaki, E. Physica, *Low Dimens. Syst. Nanostruct.* **97**, 64 (2018)
13. P. Thirumoorthy, P.K. Murali, *J. Mater. Sci. Mater. El.* **22**, 72 (2011)
14. N. Choudhury, B.K. Sarma, *Thin Solid Films* **519**, 2132 (2011)
15. K.N.K. Chidambara, S.K.B. Khadeer, G.M. Shakil, *Int. J. Chem. Tech. Res.* **7**(5), 2257 (2014–2015)
16. A.M.P. Hussain, S.N. Sarangi, S.N. Sahu, *J. Appl. Phys.* **106**, 094306 (2009)
17. R. Rai, A. Srivastava, K. Jain, *Sens. Actuators B* **138**, 304 (2009)
18. P.K. Kalita, B. Das, R. Devi, *Int. Res. J. Pure Appl. Chem* **4**(1), 97 (2014)
19. S. Jana, R. Thapa, R. Maity, K.K. Chattopadhyay, *Phys. E* **40**, 3121 (2008)
20. Z.Q. Mamiyev, N.O. Balayeva, *Opt. Mater.* **46**, 522 (2015)